

ADSORPTION ISOTHERM STUDIES ON ACID ORANGE-10 DYE REMOVAL USING CERIUM DIOXIDE NANOPARTICLES

Harry Budiman and Oman Zuas*

Research Centre for Chemistry, Indonesian Institute of Science (RCChem-LIPi),
Kawasan PUSPIPTEK Serpong, 15314 Tangerang, Banten, Indonesia

Received July 17, 2014; Accepted August 21, 2014

ABSTRACT

The adsorption capacity of AO-10 from aqueous solution onto CeO₂-NPs was investigated under various reaction parameters. Batch mode experiments were conducted to assess the potential of the CeO₂-NPs as adsorbent for the removal of AO-10 dye from aqueous solution. Equilibrium isotherm studies were carried out under an optimum reaction condition (i.e., AO-10 dye concentration = 15 mg/L, CeO₂-NPS dosage = 2 g/L, pH of dye solution = 2) obtained from this study. The equilibrium data obtained were fitted to Langmuir, Freundlich, and Redlich-Peterson isotherm models. The results shows that, the linear transform model provided the highest regression coefficient ($R^2 = 0.991$) with the Langmuir model. The maximum monolayer adsorption capacity was found to be 33.33 mg/g at 30 °C, which is higher than some data from published literature.

Keywords: dye; adsorption; isotherms; CeO₂

ABSTRAK

Kemampuan adsorpsi AO-10 dari larutan oleh CeO₂-NPs telah diteliti pada berbagai macam parameter reaksi. Eksperimen dilakukan dengan metode batch untuk mengevaluasi kemampuan CeO₂-NPs sebagai adsorben untuk penghilangan AO-10 dalam larutan. Studi kesetimbangan isotermal dilakukan pada kondisi optimum reaksi yaitu konsentrasi zat warna (AO-10 = 15 mg/L, dosis CeO₂-NPS = 2 g/L, pH larutan zat warna = 2). Data kesetimbangan yang diperoleh dicocokkan dengan model isoterm Langmuir, Freundlich dan Redlich-Peterson. Hasil menunjukkan bahwa model linear memberikan nilai koefisien regresi tertinggi ($R^2 = 0,991$) pada model Lagmuir. Kapasitas adsorpsi maksimum lapisan tunggal didapat sebesar 33,33 mg/g pada suhu 30 °C, dimana nilainya lebih tinggi dibandingkan dengan beberapa data dari literatur yang sudah terpublikasi.

Kata Kunci: zat warna; serapan; isotermal; CeO₂

INTRODUCTION

Among the aqueous environmental related issues, water pollution by synthetic dyes from industries might be one of the most serious problems. As reported in many literatures, hundred thousand tons of commercial dyes are produced annually and most of them are used by industries to color their product [1-3]. Water pollution by synthetic dyes can be occurred because high percentage of colored industrial effluents is discharged directly into aqueous environment [4-5], which further can potentially threat the aqueous ecosystem because they are aesthetic pollutants, resistant to aerobic digestion, stable to light heat and oxidizing agents, and they can hinder the light penetration required for the aqueous biological processes [6-8]. In addition, the industrial effluents containing colored textile dyes may cause toxic, carcinogenic, or mutagenic for the aquatic life. In this regards, a proper treatment of industrial effluence (waste) containing textile dye before discharge

is crucial. For the treatment purposes, numerous treatment methods have been proposed including chemical coagulation, anaerobic reduction, aerobic oxidation, membrane filtration, photo-degradation and adsorption methods [3,7-10]. Among the reported technologies, the adsorption method provides an attractive technique especially if the adsorbent has high adsorption property [11]. In this regards, non-conventional metal oxide-based adsorbent have been reported to be important materials for the removal of dyes from aqueous solution such as Mg-Fe-CO₃ layer double hydroxide [12], Cu-TiO₂ composite [13], modified magnetic silica [14], graphene oxide-F₃O₄ [15], magnetic ZnFe₂O₄ [16], and chitosan-ZnO nanoparticle [17].

Recently, Zuas et al. [18] found that CeO₂ could be potentially used as an efficient adsorbent for the removal of synthetic organic dyes in aqueous solution. In this study, the removal of AO-10 dye using CeO₂- was analyzed under different reaction parameters (i.e.,

* Corresponding author. Tel/Fax : +62-21-7560929/ 7560549
Email address : oman.zuas@lipi.go.id

changing the initial AO-10 dye concentration, changing the CeO₂-NPs dosage, changing the initial pH of the dye solution, changing the reaction time, and changing the concentration of ionic strength added in the reaction solution). However, in order to estimate practical adsorption capacity, therefore, the information on adsorption equilibrium is important. The equilibrium studies that give the capacity of both adsorbent and adsorbate are described by adsorption isotherm. In general, the adsorption isotherm is the ratio between the quantity adsorbate adsorbed on the surface of adsorbent and the remaining in solution at fixed temperature at equilibrium. The suitable isotherm model that explains the adsorption process is given separately, where the experimental data were analyzed using Langmuir, Freundlich, and Redlich Peterson isotherm.

EXPERIMENTAL SECTION

Materials

In this study, the powdered cerium dioxide nanoparticles (hereafter called CeO₂-NPs) having 10-16 nm in particles diameter was the same batch with the CeO₂-NPs used in our previous study [18]. Acid Orange-10 dye (AO-10, C₁₆H₁₀N₂O₇S₂Na₂, C.I. 16230, CAS 1936-358-4, Sigma-Aldrich) was used as a model pollutant (adsorbate) and its chemical structure is shown in Fig. 1. Acid orange is a synthetic azo dye used many staining formulation. This dye is not regarded as chronic toxic, but it can have some harmful effect including skin irritation, serious eye irritation, and respiratory irritation [19]. Deionized water (17.5 MΩ.cm of resistivity) was produced using a Milli-Q water purified system (Millipore Corp) and used in all experiment runs.

Procedure

Adsorption of AO-10 dye using CeO₂-NPs

Adsorption testing of AO-10 dye by CeO₂-NPs was conducted using batch experimental method. Typically, 0.01 g of CeO₂-NPs was transferred into 15 mL capped glass tube containing 10 mL AO-10 dye solution. Subsequently, the tube was placed in a Cetromat WR temperature-controlled water bath shaker and agitated (140 rpm) at a certain time. All of the experiments were carried out at 140 rpm at 30 °C. Afterward, supernatant solution was separated from the adsorbent by centrifugation at 2500 for 5 min using IEC Centra CL2 Thermo centrifuge. In order to determine the residue of AO-10 in solution, the absorbance of supernatant solution was measured at maximum wavelength (λ_{max}): 480 nm using Hitachi U-2000 UV-Vis spectrophotometer. Parameter of adsorption experiment including initial concentration of AO-10 dye (15-60 mg/L), adsorbent

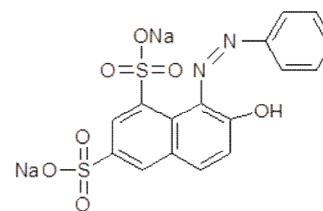


Fig 1. Chemical structure of AO-10 dye

dose (0.25–2 g/L), reaction time (1–120 min), and initial pH solution (2–10) were investigated. The pH of the AO-10 solutions were adjusted using a dilute hydrochloric acid solution (0.1 N) and sodium hydroxide solution (0.1 N). Effect of ionic strength was conducted using NaCl salt with concentration ranging from 0 to 0.7 mol/L.

Analytical measurement of AO-10 dye concentration

The concentration of residue of AO-10 dye in the solution was determined by inserting the absorbance of the AO-10 sample solutions into AO-10 calibration curve. The calibration curve of the AO-10 was made by plotting the absorbance of AO-10 standard solutions versus their concentration. A high linearity of the calibration curve was found at maximum 30 mg/L of AO-10 dye, giving an expression: $A = 0.029C - 0.011$, where A and C are the absorbance and concentration of the AO-10 standard solutions, respectively, with coefficient regression (R^2) was found to be 0.999.

The percentage removal (%-R) of the AO-10 dye was calculated using Eq. 1, while the amount of dye adsorbed at equilibrium (q_e) was calculated from the mass balance equation (Eq. 2):

$$\%R = \left(\frac{C_o - C_t}{C_o} \right) \times 100 \quad (1)$$

$$q_e = (C_o - C_e) V/m \quad (2)$$

where C_o (mg/L) is initial concentration of AO-10 dye solution, C_t (mg/L) concentration of dye after time $t_{(min)}$, C_e is the liquid phase dye concentration at equilibrium (mg/L); V is volume of dye solution used (L) and m is the mass of sorbent used (g).

pH point of zero charge

The pH point of zero charge (pH_{pzc}) of CeO₂-NPs were determined using the pH drift method [20-21]. Typically, a series of 0.01 M NaCl solution (15 mL) at different pH (2-12) were investigated. The presence of CO₂ in the solution was removed by a N₂ bubbling until a stable pH of the solution was achieved, by which this NaCl-free CO₂ solution was counted as the initial pH). After that, 15 mg of CeO₂-NPs were added into each NaCl-free CO₂ solutions and kept at room temperature for 24 h followed by measuring the pH of the solution

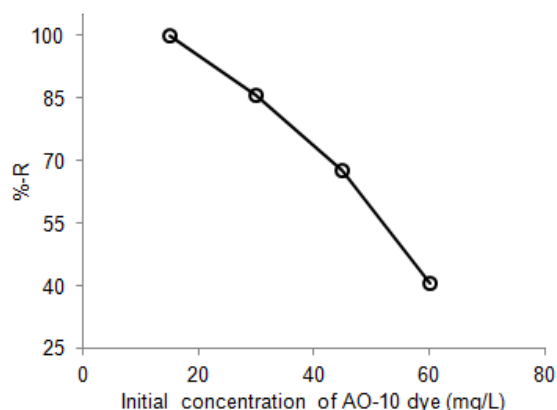


Fig 2. The effect of initial concentration of AO-10 dye on the adsorption activity of CeO₂-NPs

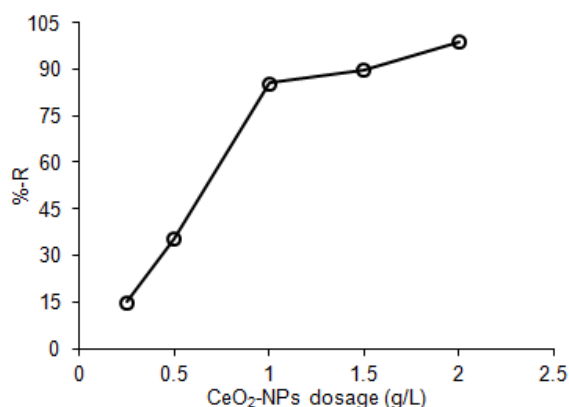


Fig 3. The effect of CeO₂-NPs dosage on the percentage removal AO-10 dyes

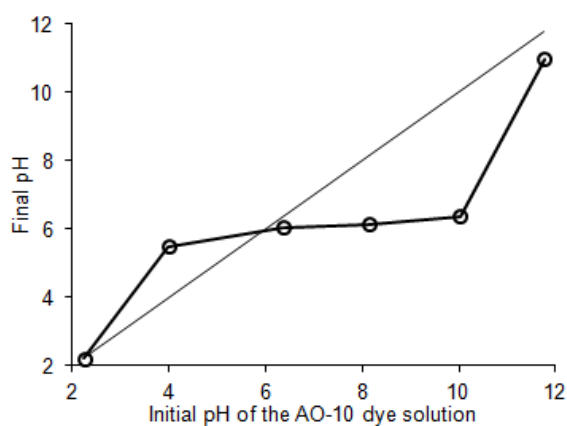


Fig 4. The pH_{pzc} of CeO₂-NPs

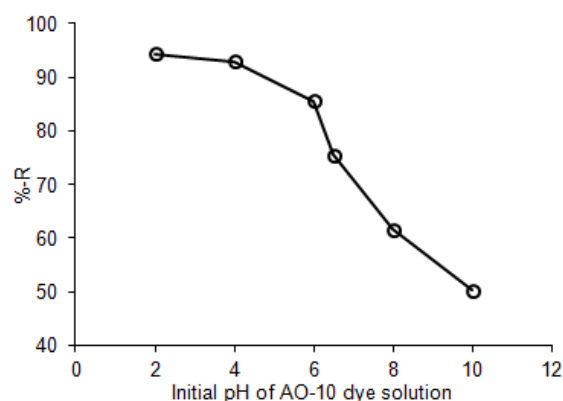


Fig 5. The effect of initial pH on the percentage removal AO-10 dye

(this measured pH values were counted as the final value). The pH_{pzc} was taken from the diagonal line of the curve of the final pH versus initial pH.

RESULT AND DISCUSSION

Effect of Reaction Parameters

Effect of initial dye concentration

The effect of initial concentration of AO-10 dye (15-60 mg/L) on CeO₂-NPs adsorption activity was studied at fixed pH 6 at 30 °C, and the result is shown in Fig. 2. As it can be seen from Fig. 2, the percentage removal of AO-10 dye decreased from 100% to 40% by increasing of AO-10 dye concentration from 15 to 60 mg/L. At the lowest concentration (15 mg/L), adsorbate molecules covered all surface active sites of CeO₂-NPs so that the highest percentage removal of dye could be obtained. On the other hands, the percentage removal of AO-10 dye decreased at higher concentration because the entire surface active sites of adsorbent were saturated by adsorbate. The fully occupation of the surface active sites by the adsorbate may delay the adsorption

process while a high amount of adsorbate molecules were remained in the bulk solution [22-23].

Effect of adsorbent dosage

The effect of adsorbent dosage on the adsorption of AO-10 dye was investigated by varying the weight of CeO₂-NPs ranging from 0.25 to 2 g/L, and the result is presented in Fig. 3. It was obviously observed from Fig. 3 that percent removal of AO-10 dye increased from 15% to 99% by increasing the dosage of CeO₂-NPs from 0.25 to 2 g/L. Increase of the adsorbent dose may contribute to the more availability of the active sites for the adsorption process [24].

Effect of initial pH

The charge of the adsorbent surface is a function of the pH of the test solution; hence, it can strongly influence the adsorbent surface toward its ability to adsorb the adsorbate from solution. It has been well-recognized that the pH point of zero charge (pH_{pzc}) is the pH at which the charge of surface adsorbent is zero [25]. The pH_{pzc} is an important characteristic for any active adsorbent as it indicates the acidity or basidity of

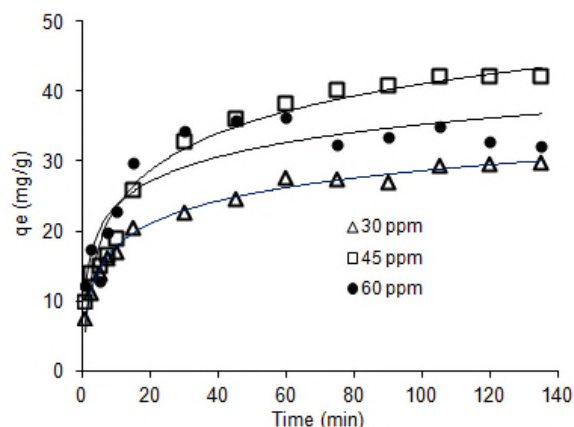


Fig 6. Time dependency of the AO-10 dye adsorption onto CeO₂-NPs

the adsorbent and net surface charge of the adsorbent in solution [25-26]. Experimentally, the pH_{pzc} of CeO₂-NPs was found to be about 6, as shown in Fig. 4. It was highlighted in previous studies [27-28] that the surface of adsorbent positively charged when $pH < pH_{pzc}$, and negatively charged when $pH > pH_{pzc}$.

Moreover, the effect of initial pH on the adsorption activity of CeO₂-NPs was investigated in the pH ranging from 2 to 10 and the result is shown in Fig. 5. From the Fig. 5, it was found that the highest percentage removal of AO-10 dye was found at pH 2 and then decreased with the increase of pH of the AO-10 dye solution. In a solution, the AO-10 dye is preferably dissociated to ion Na⁺ and sulfonate group (RSO₃⁻) with pKa value of AO-10 dye solution is 12.5 [29-30]. Consequently, the RSO₃⁻ of AO-10 dye has negative charged because the RSO₃⁻ could be protonated by H⁺ at pH difference of solution (2-10) < pKa [25-26,28]. At lower pH (acidic), the surface of adsorbent become more positively charged ($pH < pH_{pzc}$) lead to increase the percentage removal due to strengthening the attractive forces between adsorbate and adsorbent. On the other hands, the surface of adsorbent become more negatively charge along with the increase of pH solution ($pH > pH_{pzc}$) lead to decrease the adsorption ability of adsorbent. This decrease phenomenon was due to stronger of the repulsion forces between adsorbate and adsorbent.

Effect of adsorption time

Fig. 6 shows a time dependency of the adsorption at difference of AO-10 dye concentration. As can be seen from Fig. 6, the adsorption of AO-10 dyes was found to increase with time and achieved its equilibrium after 120 min. Typically, the adsorption of AO-10 dye was rapidly occurred at the first 20 min which was probably due to the presence of large amount accessible surface active sites on CeO₂-NPs. After that, the rate of adsorption process was slowly increasing. This slow increase might be due to huge number of surface active

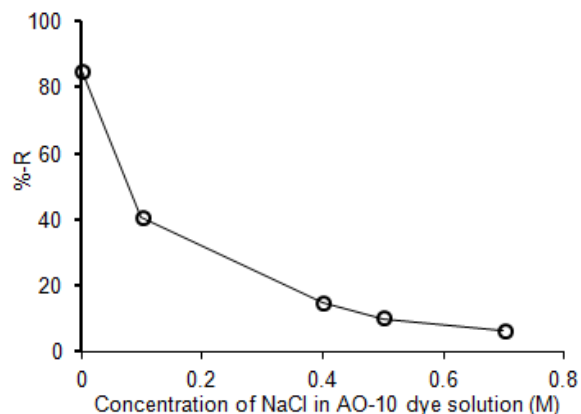


Fig 7. Effect of ionic strength on the adsorption of AO-10 dye onto CeO₂-NPs

sites have been covered by the AO-10 dye molecules, where this condition induces the occurrence of the repulsion forces between adsorbate at solid-solution interface [16,23]. Moreover, no considerable change on the amount of AO-10 dye adsorbed after 120 min, suggesting that the equilibrium process has been achieved.

Effect of ionic strength

Fig. 7 demonstrates the effect of ionic strength on the adsorption of AO-10 dye onto CeO₂-NPs. It can be observed from Fig. 7 that the percentage removal of AO-10 dye decreased with increasing the concentration of NaCl in solution. In the solution, the Na⁺ ions originated from NaCl has not only neutralized the negative charge of RSO₃⁻ group in AO-10 dye, but also results more positive charge of the surface of CeO₂-NPs. Such conditions were responsible to reduce the attractive forces between adsorbate molecules and adsorbent. This phenomenon in line with the assumption that the increase of ionic strength by the existence of NaCl in the solution may cause decrease the adsorption capacity of the adsorbate when an attractive of electrostatic interaction is occurred between adsorbate and adsorbent [16].

Adsorption Isotherm

Adsorption isotherm study is essential for investigating the interaction mechanism between adsorbate and adsorbent, which further beneficially in evaluating the efficiency of the adsorbent for adsorbate removal. The adsorption isotherm indicates the relationship between the adsorbate in the liquid phase and the adsorbate adsorbed on the surface of the adsorbent at equilibrium at constant temperature. In this study, the adsorption isotherm was evaluated using Langmuir, Freundlich, and Redlich Peterson model.

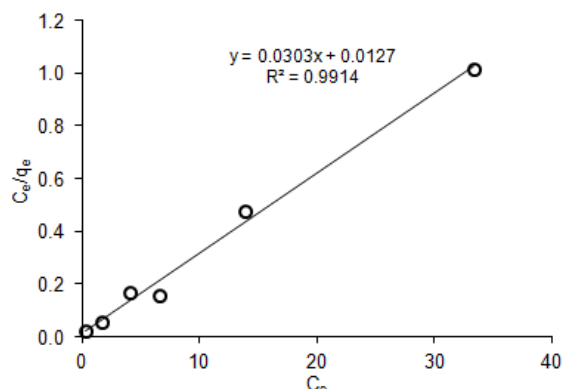


Fig 8. Langmuir isotherm model for the adsorption of AO-10 dye onto CeO₂-NPs

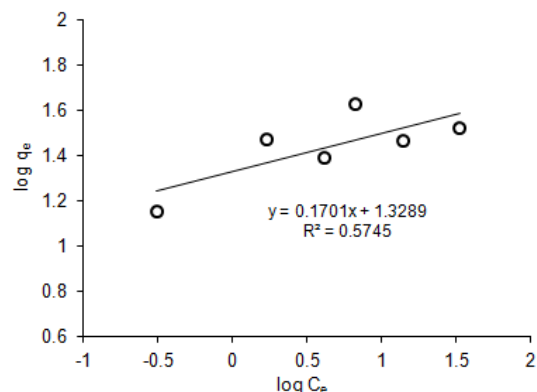


Fig 9. Freundlich isotherm curve for the adsorption of AO-10 dye onto CeO₂-NPs

Table 1. Isotherm constant of the models for the adsorption of AO-10 dye onto CeO₂-NPs

Langmuir isotherm		Freundlich isotherm		Redlich -Peterson isotherm	
Parameter	Value	Parameter	Value	Parameter	Value
Q ₀ (mg/g)	33.333	K _F (mg/g)/(L/mg) ⁿ	21.281	K _{rp} (L/g)	67.12
b (L/mg)	2.5	n	5.882	α (L/mg)	1.683
R ²	0.991	R ²	0.574	β	1.065
				R ²	0.988

Langmuir isotherm

Langmuir isotherm is an adsorption model. This isotherm model takes an assumption that the monolayer adsorption occurs at specific homogenous sites within the adsorbent, which expressed by the Eq. (3).

$$q_e = \frac{Q_0 b C_e}{1 + b C_e} \quad (3)$$

where q_e (mg/g) is the amount of dye adsorbed per unit mass of adsorbent, C_e (mg/L) is the concentration of AO-10 dye remaining in the solution after equilibrium. Q_0 is the maximum amount of required to form a complete monolayer on the adsorbent surface at high C_e . The b is the constant related to the affinity of the binding sites (L/mg). The linear equation of the Langmuir model can be expressed by Eq. (4).

$$\frac{C_e}{q_e} = \frac{1}{Q_0 b} + \frac{C_e}{Q_0} \quad (4)$$

Fig. 8 shows the linear graphics of specific adsorption (C_e/q_e) against the equilibrium concentration (C_e). This relationship clarifies that the adsorption of AO-10 dye on the surface of CeO₂-NP is in agreement with the Langmuir model. The Langmuir constant, Q_0 and b were determined from the slope and intercept of the linear plot of Fig. 8. The important characteristic of Langmuir isotherm is a dimensionless constant separation (R_L) which is expressed in the Eq. (5).

$$R_L = \frac{1}{(1 + b C_0)} \quad (5)$$

where C_0 is the highest initial concentration of adsorbate (mg/L), and b is the constant of Langmuir. The shape of Langmuir isotherm is indicated by the value of R_L

includes unfavorable ($R_L > 1$), linear ($R_L = 1$), favorable ($0 < R_L < 1$), or irreversible ($R_L = 0$) [31]. In this study, the value of R_L was found to be 0.00662, demonstrating that the shape of Langmuir isotherm model for the adsorption of AO-10 dye onto CeO₂-NPs is favorable. Parameters characteristic of the Langmuir isotherm model obtained in this study are listed in Table 1.

Freundlich isotherm

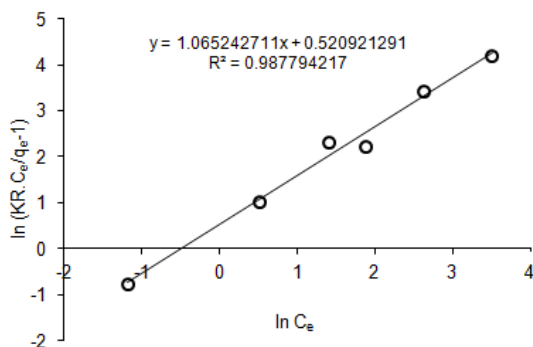
Freundlich isotherm is an empirical equation for describing single-component adsorption on heterogeneous surfaces due to the variation of functional group presence in the surface. Consequently, the interaction between adsorbate and adsorbent is occurred at different affinity [31-32]. The equation of the Freundlich isotherm model is given by the Eq. (6).

$$q_e = K_f C_e^{1/n} \quad (6)$$

where K_f and n are Freundlich constants. The K_f (mg/g (L/mg)^{1/n}) is the adsorption capacity of the sorbent, in which the value of n denotes the favorable of the adsorption process, while value of $1/n$ (0 to 1) showed the criterion of adsorption intensity or the heterogeneous of the adsorbent surface. The more heterogenic of the adsorbent surface the more favorable of the adsorption condition for Freundlich model. Under this condition, the value of $1/n$ approach to 0. The linear plot (Eq. 7) describing the relationship between $\log q_e$ versus $\log C_e$ is subjected to determine the K_f constant and n [23,31-32].

Table 2. A maximum monolayer of various adsorbents for AO-10 dye adsorption

Adsorbents	Q ₀ (mg/g)	T (°C)	Reference
CeO ₂ -NPs	33.33	30	This study
<i>Thespesia populnea</i> pods carbon	9.13	25	[34]
Bagasse fly ash	18.80	30	[30]
Saw dust	0.4045	35	[35]
Mg-Fe-CO ₃ layer double hydroxide	72.08	25	[12]
Monoamine modified magnetic silica	60.02	25	[14]
Waste sugarcane bagasse carbon	3.92	40	[36]

**Fig 10.** Redlich-Peterson isotherm for the adsorption of AO-10 dye onto CeO₂-NPs

$$\log q_e = \log K_f + \left(\frac{1}{n}\right) \log C_e \quad (7)$$

The value of K_f and n are listed in Table 1, which was calculated from the intercept and the slope of the linear graphic of the Fig. 9.

Redlich Peterson isotherm

Redlich-Peterson isotherm is the adsorption model which is used to compromise the limitation of both the Langmuir and Freundlich isotherm models. Thus, the equation of the Redlich-Peterson model combines parameters from the Langmuir and Freundlich model. The adsorption mechanism of Redlich-Peterson model follows a non ideal monolayer adsorption that is a hybrid mechanism from the Langmuir and Freundlich isotherm [28,33]. Redlich-Peterson model is expressed by the Eq. 8.

$$q_e = \frac{K_{rp} C_e}{1 + \alpha C_e^\beta} \quad (8)$$

where q_e is the amount of adsorbate adsorbed per unit mass of adsorbent (mg/g), C_e is the adsorbate concentration remained in solution after equilibrium (mg/L). The Redlich-Peterson isotherm constants including K_{rp} (L/g), α (L/mg), and β can be determined from the Eq. 8. The β value is exponential value range from 0 to 1. Adsorption model follows the Langmuir model when the β value is 1, while when the β value is 0, the adsorption model follows the Henry's law.

The linear graphic of Redlich-Peterson is given by the following equation (Eq. 9).

$$\ln\left(\frac{K_{rp} C_e}{q_e} - 1\right) = \beta \ln(C_e) + \ln(\alpha) \quad (9)$$

The values of K_{rp} , α , and β were calculated from intercept and slope of the linear plot in the Fig. 10 and the results are listed in Table 1. Based on the data as listed in Table 1, correlation coefficient of isotherm Langmuir model (R^2 : 0.991) is higher than Freundlich and Redlich-Peterson model, indicating that the adsorption of AO-10 dye onto CeO₂-NPs had good agreement with the Langmuir isotherm. Thus, it can be suggested that the AO-10 dye was adsorbed on the homogenous surface active site of adsorbent via a development of monolayer adsorbate mechanism. The adsorption capacity of monolayer generated by the Langmuir model was found to be 33.33 mg/g at 30 °C

Table 2 compares the adsorption capacities of the synthesized CeO₂-NPs with various types of adsorbent for AO-10 dye removal. As can be seen, the adsorption capacity of CeO₂-NPs for AO-10 adsorption is 33.33 mg/g, which was higher than *Thespesia populnea* pods carbon, bagasse fly ash, saw dust, and waste sugarcane bagasse carbon. On the other hands, the value of Q_0 of CeO₂-NP is smaller than Mg-Fe-CO₃ layer double hydroxide and monoamine modified magnetic silica (MAMMS). This finding indicates that the CeO₂-NPs was more efficient as adsorbent for AO-10 dye removal than other as listed in Table 1, except for Mg-Fe-CO₃ and monoamine modified magnetic silica (MAMMS) adsorbent.

CONCLUSION

In this study, CeO₂-NP was found as an active material for removing AO-10 dye from aqueous water using batch system. Percentage removal of AO-10 dye was highly affected by the parameter reaction used. The favor condition for the adsorption of AO-10 dye was found at initial pH 2, giving 94% percentage removal. It was observed that the adsorption of capacity follows Langmuir isotherm type with 33.33 mg/g maximum monolayer adsorption capacity.

REFERENCES

1. Priya, M.S., Divyashree, K., Goswami, C., Prabha, M.L., and Babu, A.K.S., 2013, *Int. J. Eng. Adv. Technol.*, 2 (4), 913–918.
2. Pavanelli, S.P., Bispo, G.L., Nascentes, C.C., and Augusti, R., 2011, *J. Braz. Chem. Soc.*, 22 (1), 111–119.
3. Annadurai, G., Juang, R.S. and Lee, D.J., 2002, *J. Hazard. Mater.*, B92, 263–274.
4. Olaniyi, I., Raphaeel, O., and Onyebuchi, N.J., 2012, *Arch. Appl. Sci. Res.*, 4 (1), 406–413.
5. Rasul, M.G., Faisal, I., and Khan, M.M.K., 2006, *Int. J. Environ. Pollut.*, 28 (1-2), 144–161.
6. Namasivayam, C., Radhika, R., and Suba, S., 2001, *Waste Manage.*, 21 (4), 381–387.
7. Hariharan, C., 2006, *Appl. Catal., A*, 304, 55–61.
8. Sun, Q., and Yang, L., 2003, *Water Res.*, 37 (7), 1535–1544.
9. Nigam, P., Banat, I.M., Singh, D., and Marchant, R., 1996, *Proc. Biochem.*, 31 (5), 435–442.
10. Pandit, P., and Basu, S., 2004, *Ind. Eng. Chem. Res.*, 43 (24), 7861–7864.
11. Masykur, A., Santosa, S.J., Siswanta, D., and Jumina, 2014, *Indo. J. Chem.*, 14 (1), 63–70.
12. Abdelkader, N.B-H., Bentouami, A., Derriche, Z., Bettahar, N., and de Ménorval, L.-C., 2011, *Chem. Eng. J.*, 169 (1-3), 231–238.
13. Zuas, O., and Budiman, H., 2013, *Nano-Micro Lett.*, 5 (1), 26–33.
14. Atia, A.A., Donia, A.M., and Al-Amrani, W.A., 2009, *Chem. Eng. J.*, 150 (1), 55–62.
15. Meral, K., and Metin, O., 2014, *Turk. J. Chem.*, 1–8.
16. Konicki, W., Sibera, D., Mijowska, E., Lendzion-Bieluń, Z., and Narkiewicz, U., 2013, *Colloid Interface Sci.*, 398, 152–160.
17. Salehi, R., Arami, M., Mahmoodi, N.M., Bahrami, H., and Khorramfar, S., 2010, *Colloids Surf., B*, 80 (1), 86–93.
18. Zuas, O., Abimanyu, H., and Wibowo, W., 2014, *Proc. Appl. Ceram.*, 8 (1), 39–46.
19. AMRESO Safety Data Sheet of Acid Orange 10, 2014, <http://www.amresco-inc.com/media.acux?path=/media/products/msds/MSDS-E783.pdf>, accessed on 4 June 2014.
20. Lopez-Ramon, F.M., Stoeckli, V., Moreno-Castilla, C., and Carrasco-Marin, F., 1999, *Carbon*, 37 (8), 1215–1221.
21. Al-Dege, Y.S., El-Barghouthi, M.I., El-Sheikh, A.H., and Walker, G.M., 2008, *Dyes Pigm.*, 77 (1), 16–23.
22. Khezami, L., and Capart, R., 2005, *Hazard. Mater.*, 123 (1-3), 223–231.
23. Ghaedi, M., Heidarpoor, Sh., Kokhdan, S.N., Sahraie, R., Daneshfar, A., and Brazesh, B., 2012, *Powder Technol.*, 228, 18–25.
24. Garg, V.K., Gupta, R., Yadav, A.B., and Kumar, R., 2003, *Bioresour. Technol.*, 89 (2), 121–124.
25. Khare, P., and Kumar, A., 2012, *Appl. Water Sci.*, 2 (4), 317–326.
26. Dursun, G., Çiçek, H., and Dursun, A.Y., 2005, *J. Hazard. Mater.*, 125 (1-3), 175–182.
27. Dąbrowski, A., Podkościelny, P., Hubicki, Z., and Barczak, M., 2005, *Chemosphere*, 58 (8), 1049–1070.
28. Liu, Q.-S., Zheng, T., Wang, P., Jiang, J.-P., and Li, N., 2012, *Chem. Eng. J.*, 157 (2-3), 348–356.
29. Cheung, W.H., Szeto, Y.S., and McKay, G., 2009, *Bioresour. Technol.*, 100 (3), 1143–1148.
30. Mall, I.D., Srivastava, V.C., and Agarwal, N.K., 2006, *Dyes Pigm.*, 6 (3), 210–223.
31. Tan, L.A.W., Ahmad, A.L., and Hameed, B.H., 2009, *J. Hazard. Mater.*, 164 (2-3), 473–482.
32. Hameed, B.H., and El-Khaiary, M.I., 2008, *J. Hazard. Mater.*, 157 (2-3), 344–351.
33. Ho, Y.-S., Malarvizhi, R., and Sulochana, N., 2009, *J. Environ. Prot. Sci.*, 3, 111–116.
34. Arulkumar, M., Sathishkumar, P., and Palvannan, T., 2011, *J. Hazard. Mater.*, 186 (1), 827–834.
35. Singh, J., Uma, Mishra, N. S., Banerjee, S., Gusain, D., and Sharma, Y.C., 2011, *Appl. Sci. Environ. Sanit.*, 6 (3), 2732–2743.
36. Tsai, W.T., Chang, C.Y., Lin, M.C., Chien, S.F., Sun, H.F., and Hsieh, M.F., 2011, *Chemosphere*, 45 (1), 51–58.